Pasture Appendix

Mapbiomas 10m - Collection 3

Version 1

General coordinator
Laerte Guimarães Ferreira Jr.
Technical coordinator
Vinicius Vieira Mesquita
Ana Paula Matos

Team
Ana Paula Carlos Assunção
Leandro Parente
Luís Bauman
Mariana Gomes
Nathalia Teles
Tharles Andrade
Wilton Ladeira da Silva

April, 2026

1. Introduction

Pastureland is the dominant human-driven land use in Brazil, currently covering approximately 164 million hectares, or about 19% of the national territory (MapBiomas, 2024). Historically, the conversion of native vegetation into pastures has been the primary engine of land use and land cover (LULC) changes across the country. Between 1985 and 2023, pasture areas in Brazil grew by approximately 78%, expanding from 92 million hectares to its current extent. This expansion was marked by a significant geographical shift, moving from consolidated regions in the Atlantic Forest and Southern grasslands toward the Cerrado and Amazon biomes (Parente et al., 2019; MapBiomas, 2024).

In the context of Brazilian territorial dynamics, pasturelands act as "land reservoirs", a transitional stage and a strategic stock of land following the initial conversion of native vegetation. These areas often serve as a placeholder for future intensification processes, eventually being converted into croplands like soy and corn (Brandão et al., 2006; Macedo et al., 2012). While pastures are vital to the national economy, supporting one of the world's largest commercial cattle herds and contributing significantly to the total Brazilian GDP (the livestock chain accounted for approximately 7% of the national GDP (CNA/CEPEA, 2024), they also present critical environmental challenges, acting as the main precursor to deforestation (Alencar, 2022).

Currently, the Brazilian landscape exhibits a dual trend: retraction in consolidated regions, particularly in the Southeast and South-Central areas, where pastures are being replaced by mechanized agriculture (Cohn et al., 2014; Zalles et al., 2019), and an expansion in native vegetation "hotspots" in the Matopiba region (the Cerrado frontier) and the new Amazonian frontier known as AMACRO, a strategic development zone encompassing the intersection of Acre, Amazonas, and Rondônia (Maciel ,2025).

Using data from ESA's Sentinel-2 constellation at 10-meter resolution for the period of 2016 to 2024, the MapBiomas 10 meter Collection 3 of pasture maps follows the general methodological approach established by Parente et al. (2019). However, this collection incorporates specific refinements focused on ensuring a resolution leap, allowing for higher precision in pastureland detection within complex landscapes, such as wooded savannas and highly fragmented rural mosaics.

In alignment with the principles of transparency and open science, all processing scripts and classification algorithms used in this methodology are publicly available and the codebase can be accessed at the official MapBiomas Pasture GitHub repository: https://github.com/mapbiomas/brazil-pasture.

2. Methodological description

The production of pasture maps for Brazil in this collection is based on the methodology established by Parente et al. (2019), which utilizes a regionalized supervised

classification approach, which integrates ESA Sentinel-2 data, robust training samples, and the Random Forest (RF) machine learning algorithm to handle the high dimensionality of the feature space (Figure 1).

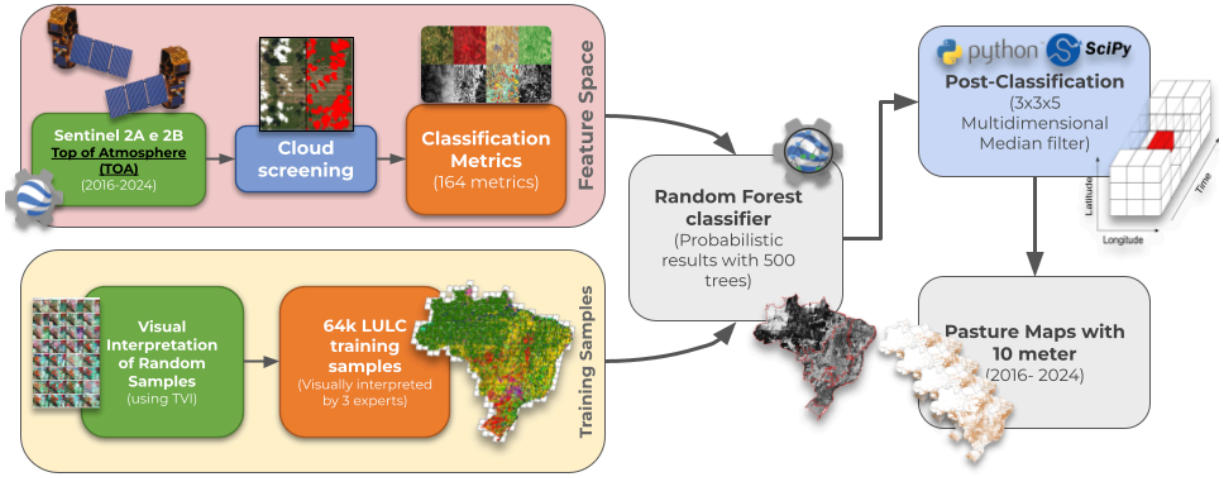

Figure 1 - Pasture mapping workflow regarding the MapBiomas 10 m Collection 3.

With a broad option of spectral bands, ESA'S Harmonized Sentinel-2 MSI *Top of Atmosphere* data, stored in Earth Engine Platform, A new, expanded feature space was constructed, maintaining the core features described by Parente et al. (2019) while incorporating advanced metrics made possible by the higher spectral resolution of the Sentinel-2 sensors.

A significant advancement in the MapBiomas 10 meter collection is the inclusion of the Red Edge spectral region (Bands 5, 6, and 7). These bands are highly sensitive to chlorophyll content and leaf structure, making them crucial for distinguishing between healthy pasture, senescent vegetation, and native physiognomies. Furthermore, the inclusion of these bands allowed for the calculation of specialized spectral indices. Notably, the Soil-Adjusted Total Vegetation Index (SATVI) was incorporated to improve the detection of dry biomass and senescent grasslands, which are often confused with bare soil or degraded areas in traditional indices like NDVI (Marsett et al., 2006).

ESA Sentinel 2 - MSI sensors (MultiSpectral Instrument) deliver the Red Edge spectral region, which are highly sensitive to chlorophyll content and leaf structure, making them crucial for distinguishing between healthy pasture, senescent vegetation, and native physiognomies. Furthermore, the inclusion of these bands allowed for the calculation of specialized spectral indices, like Soil-Adjusted Total Vegetation Index - SATVI (Marsett et al., 2006), improves the detection of dry biomass and senescent pasturelands, which are often confused with bare soil or degraded areas in traditional indices like NDVI (Marsett et al., 2006).

In total, 164 metrics were used as the feature space for this collection (Table 1). This represents a significant increase from previous iterations, adding 88 new metrics to the 76

originally used in the MapBiomas 30m series (Collection 10). These metrics include temporal statistics (min, max, median, and amplitude) of spectral bands and indices.

Table 1. Table showing the feature space used in the pasture mapping with Sentinel 2 constellation, composed of 162 spectral-temporal metrics (Sentinel 2 based) and 2 time independent metrics (SRTM data).

Bands/Indexes	Reducers
Blue (B2)	Minimum, Median, Maximum, Amplitude, Standard Deviation, Percentile (10%,25%,75%,90%)
Green (B3)	
Red (B4)	
Red Edge 1 (B5)	
Red Edge 2 (B6)	
Red Edge 3 (B7)	
Near Infrared	
Red Edge 4 (B8A)	
Short Wave Infrared 1 (B11)	
Short Wave Infrared 2 (B12)	
Normalized Difference Vegetation Index - **NDVI** (Tucker et al., 1979)	
Normalized Difference Water Index - **NDWI** (Gao, 1996)	
Cellulose Absorption Index - **CAI** (Nagler et al., 2000)	
Carotenoid Reflectance Index - **CRI1** (Gitelson et al., 2002)	
Anthocyanin Reflectance Index - **ARI1** (Gitelson et al., 2001)	
Simple Ratio Red/Green Red-Green Ratio - **RGR** (Gamon and Surfus, 1999)	
Plant Senescence Reflectance Index - **PSRI** (Merzlyak et al., 1999)	
Soil-Adjusted Total Vegetation Index - **SATVI** (Marsett et al., 2006)	
SRTM - **Elevation** (Farr et al., 2007)	-
SRTM - **Slope** (Farr et al., 2007)	-

In Collection 3, like shown in Table 2, a strategic decision was made to exclude Latitude and Longitude bands from the feature space. Previous iterations (MapBiomas 30m series - Collection 9) revealed that the Random Forest model was developing a spatial bias, where the coordinate bands introduced artificial gradient anomalies and "staircase" effects in the pasture probability predictions. By removing these geographical variables, the model was forced to rely strictly on the bio-optical properties of the targets, resulting in a more consistent classification.

Table 2 . Overview of Pasture mapping approach through 10 meter collections

Collection	Time Interval	Method	Key Improvements
1	2016-2022	Random Forest	
2	2016-2023	Random Forest	- Inclusion of ~4.600 intervention samples
3	2016-2024	Random Forest	- Removal of latitude and longitude metrics - Added 10.000 random stratified training samples sorted over Mosaic of Uses cluster cores from 30 meter Collection 9

The Random Forest classifier (Breiman, 2001) training considered the same 60,000 random samples visually interpreted by experts using TVI (MapBiomas 30m Collection 10) plus 4,718 intervention points, used to ensure that the classifier will not fail to detect pasture areas not covered by the main sampling approach. Furthermore, the classifier hyperparameters were kept the same, except for the number of variables per split, which follows the square root value of the feature space size (approximately 13).

The region design followed a different approach compared to the Landsat WRS seamless scene chosen by Parent et al. (2019), here we considered the standard IBGE 1:250.000 (160 km x 100 km) Topographic Charts (Figure 2). This region division was selected because the Sentinel 2 grid division follows a Military Grid Reference System (MGRS), usually composed of a 100 km x 100 km tilling system, which doesn't match with the real image dimension and format.

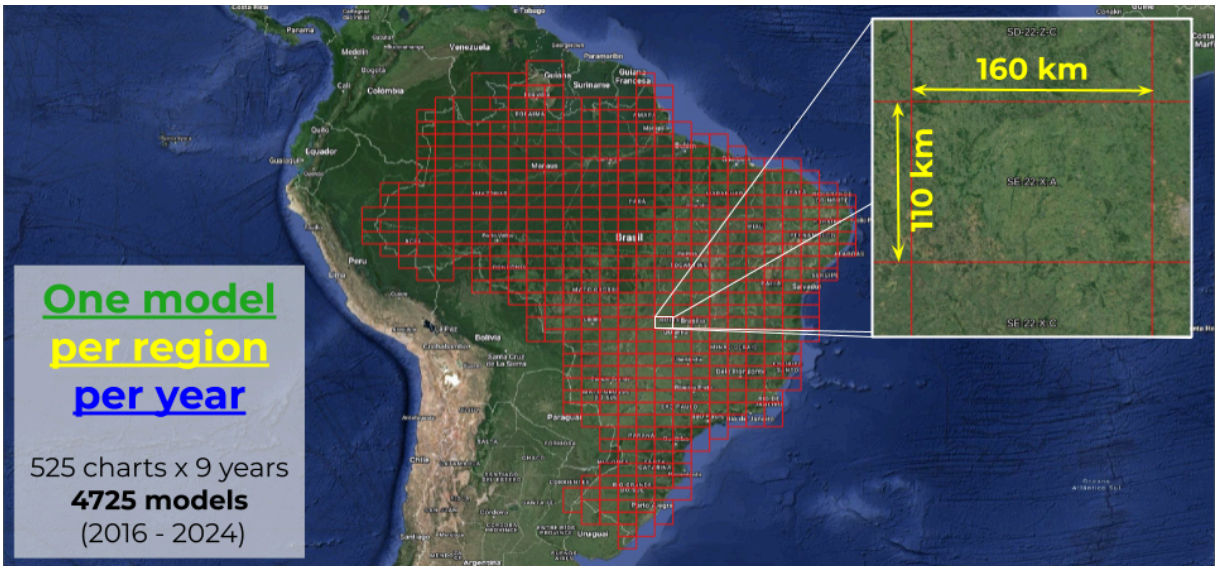

Figure 2 - Representation of IBGE 1:250.000 Topographic Charts used as regions in

classification schema and the aggregated number of models trained (4752 models) by year, by region and by year.

3. Post-processing

The spatiotemporal filter used in the probabilistic pasture maps, before collection integration, was kept the same as in the other MapBiomas collections due to its simplicity and quality of results, which are even superior to some complex 3D Savitzky-Golay filters. It consists of a simple multidimensional median filter with a 3 x 3 window in space (X and Y) for 5 years (Z) packed in the Scipy library from the Python language (Figure 3). After the filtering process, the maps are transformed from probabilistic maps to discrete maps by establishing the cut-off point for pasture areas for probabilities greater than 51%.

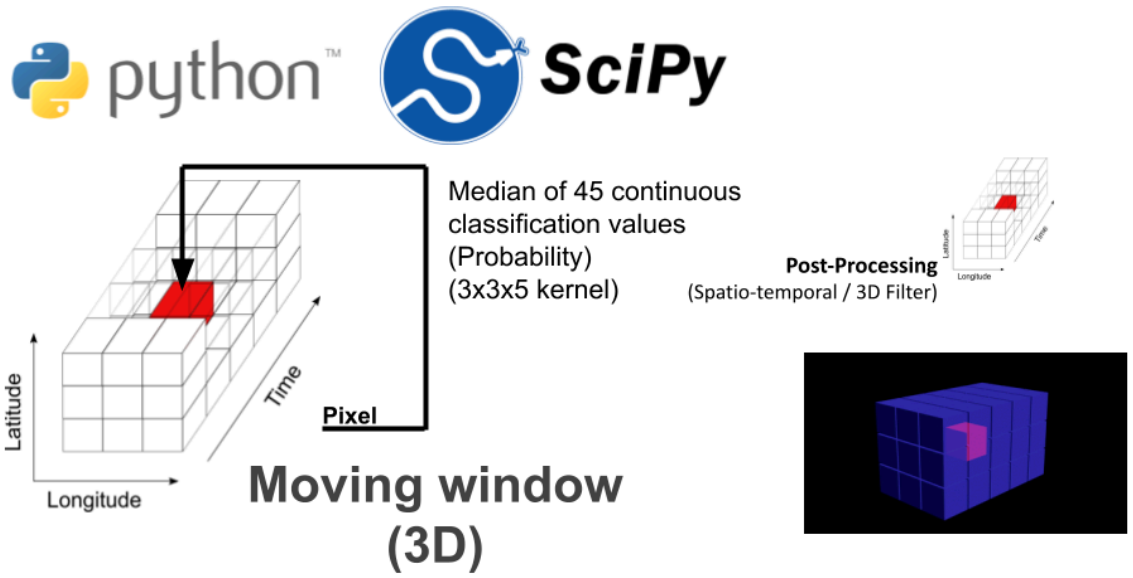

Figure 3 - Schematic representation of the 3D Moving Window concept using the SciPy library in Python to perform non-destructive gap filling and probability smoothing in pasture maps.

4. Known Limitations And Advantages

Compared to classification approaches utilizing Landsat series data (MapBiomas 30m), the use of Sentinel-2 data with 10m spatial resolution enabled a sharper delimitation of pasture areas, yielding results with greater spatial consistency. Also, the 5-day revisit cycle provided by two satellites (2A and 2B) enhanced the pasture detection capabilities by providing a larger and more consistent volume of data per pixel. However, improvements in spatial and temporal resolution carries certain trade-offs, such as increased information density and variability, alongside a significant rise in computational and storage requirements. Limitations observed across both collections include: the misclassification of cropland areas as pasture, and the misclassification of short natural vegetation as pasture in the northern Amazon region (partially solved in Collection 3).

5. References

Alencar, A. A. C., Arruda, V. L. S., Silva, W. V. da, Conciani, D. E., Costa, D. P., Crusco, N., Duverger, S. G., Ferreira, N. C., Franca-Rocha, W., Hasenack, H., Martenexen, L. F. M., Piontekowski, V. J., Ribeiro, N. V., Rosa, E. R., Rosa, M. R., dos Santos, S. M. B., Shimbo, J. Z., & Vélez-Martin, E. (2022). Long-term Landsat-based monthly burned area dataset for the Brazilian biomes using deep learning. Remote Sensing, 14(11), 2510. https://doi.org/10.3390/rs14112510

Brandão, A. S. P., Rezende, G. C. de, & Marques, R. W. da C. (2006). Crescimento agrícola no período 1999/2004: a explosão da soja e da pecuária bovina e seu impacto sobre o meio ambiente. Economia aplicada, 10(2), 249–266. https://doi.org/10.1590/s1413-80502006000200006

Breiman, L. (2001). Random forests. Machine Learning, 45(1), 5–32. https://doi.org/10.1023/a:1010933404324

Cohn, A. S., Mosnier, A., Havlík, P., Valin, H., Herrero, M., Schmid, E., O'Hare, M., & Obersteiner, M. (2014). Cattle ranching intensification in Brazil can reduce global greenhouse gas emissions by sparing land from deforestation. Proceedings of the National Academy of Sciences of the United States of America, 111(20), 7236–7241. https://doi.org/10.1073/pnas.1307163111

Farr, T. G., Rosen, P. A., Caro, E., Crippen, R., Duren, R., Hensley, S., Kobrick, M., Paller, M., Rodriguez, E., Roth, L., Seal, D., Shaffer, S., Shimada, J., Umland, J., Werner, M., Oskin, M., Burbank, D., & Alsdorf, D. (2007). The Shuttle Radar Topography Mission. Reviews of Geophysics (Washington, D.C.: 1985), 45(2). https://doi.org/10.1029/2005rg000183

Gamon, J. A., & Surfus, J. S. (1999). Assessing leaf pigment content and activity with a reflectometer. The New Phytologist, 143(1), 105–117. https://doi.org/10.1046/j.1469-8137.1999.00424.x

Gao, B. C. (1996). NDWI--a normalized difference water index for remote sensing of vegetation liquid water from space. Remote Sensing of Environment, 58(3), 257–256. https://doi.org/10.1016/s0034-4257(96)00067-3

Gitelson, A. A., Kaufman, Y. J., Stark, R., & Rundquist, D. (2002). Novel algorithms for remote estimation of vegetation fraction. Remote Sensing of Environment, 80(1), 76–87. https://doi.org/10.1016/s0034-4257(01)00289-9

Gitelson, A. A., Merzlyak, M. N., & Chivkunova, O. B. (2001). Optical properties and nondestructive estimation of anthocyanin content in plant leaves¶. Photochemistry and Photobiology, 74(1), 38. https://doi.org/10.1562/0031-8655(2001)074<0038:opaneo>2.0.co;2

Macedo, M. N., DeFries, R. S., Morton, D. C., Stickler, C. M., Galford, G. L., & Shimabukuro, Y. E. (2012). Decoupling of deforestation and soy production in the southern Amazon during the late 2000s. Proceedings of the National Academy of Sciences of the United States of America, 109(4), 1341–1346. https://doi.org/10.1073/pnas.1111374109

Maciel, E. (2025, outubro 5). AMACRO se consolida como novo epicentro do desmatamento na Amazônia. BNC Amazonas, o site de política!; BNC Amazonas. https://bncamazonas.com.br/municipios/amacro-se-consolida-como-novo-epicentro-do-desmatamento-na-amazonia/

Marsett, R. C., Qi, J., Heilman, P., Biedenbender, S. H., Carolyn Watson, M., Amer, S., Weltz, M., Goodrich, D., & Marsett, R. (2006). Remote sensing for grassland management in the arid southwest. Rangeland Ecology & Management, 59(5), 530–540. https://doi.org/10.2111/05-201r.1

Merzlyak, M. N., Gitelson, A. A., Chivkunova, O. B., & Rakitin, V. Y. U. (1999). Non-destructive optical detection of pigment changes during leaf senescence and fruit ripening. Physiologia Plantarum, 106(1), 135–141. https://doi.org/10.1034/j.1399-3054.1999.106119.x

Nagler, P. L., Daughtry, C. S. T., & Goward, S. N. (2000). Plant litter and soil reflectance. Remote Sensing of Environment, 71(2), 207–215. https://doi.org/10.1016/s0034-4257(99)00082-6

Parente, L., Mesquita, V., Miziara, F., Baumann, L., & Ferreira, L. (2019). Assessing the pasturelands and livestock dynamics in Brazil, from 1985 to 2017: A novel approach based on high spatial resolution imagery and Google Earth Engine cloud computing. Remote Sensing of Environment, 232(111301), 111301. https://doi.org/10.1016/j.rse.2019.111301

PIB do agronegócio fecha 2024 com crescimento de 1,81%. (s. d.). Portal CNA Brasil. Recuperado 25 de abril de 2026, de https://www.cnabrasil.org.br/noticias/pib-do-agronegocio-fecha-2024-com-crescimento-de-1-81

Tucker, C. J., Elgin, J. H., McMurtrey, J. E., Iii, & Fan, C. J. (1979). Monitoring corn and soybean crop development with hand-held radiometer spectral data. Remote Sensing of Environment, 8(3), 237–248. https://doi.org/10.1016/0034-4257(79)90004-x

Zalles, V., Hansen, M. C., Potapov, P. V., Stehman, S. V., Tyukavina, A., Pickens, A., Song, X.-P., Adusei, B., Okpa, C., Aguilar, R., John, N., & Chavez, S. (2019). Near doubling of Brazil's intensive row crop area since 2000. Proceedings of the National Academy of Sciences of the United States of America, 116(2), 428–435. https://doi.org/10.1073/pnas.1810301115